

CHAPTER 37

AN EFFICIENT METHOD FOR THE REPRODUCTION OF NON-LINEAR RANDOM WAVES

Gert Klopman ¹ and Peter Jan Van Leeuwen ²

Abstract

For the laboratory study of many random-wave induced phenomena, wave-board control signals according to linear wave theory are not sufficient: apart from bound sub- and superharmonic waves, spurious free waves are generated. Wave generation according to a higher-order wave theory is necessary in order to suppress these spurious waves. The perturbation method of multiple scales is used to derive formulas for the second-order wave-board control signal, assuming the carrier-wave spectrum is narrow banded. The resulting algorithm is much faster than the one based on the full second-order theory. Furthermore, the applicability of the narrow-band approximation is indicated for carrier-wave spectra frequently used in coastal and ocean engineering.

1 Introduction

For the extrapolation of laboratory data to full scale sea conditions it is essential to have a realistic reproduction of the sea in laboratory experiments. In a natural wave train, with the spectral energy density concentrated around the peak frequency, the non-linearity of the free-surface boundary conditions introduces sub- and superharmonics which are phase locked to the primary wave components. When the system under investigation is perceptible to these sub- and superharmonics, it is important to reproduce them correctly in the laboratory.

The subharmonics (or bound long waves) can generate the forcing for long-period harbour oscillations, slow-drift motions of moored vessels and tension-leg platforms, and offshore sand-bar formation due to sediment transport. The superharmonics introduce sharper-peaked wave crests and flatter troughs, they are important for sediment transport due to wave asymmetry and can be of importance for forces on offshore structures.

¹Delft Hydraulics, P.O. Box 152, 8300 AD Emmeloord, The Netherlands.

²Delft University of Technology, Dept. of Civil Engineering, P.O. Box 5048, 2600 GA Delft, The Netherlands.

An incorrect (linear) reproduction in the laboratory generates free waves at the same frequencies as the bound sub- and superharmonics, but travelling at a different speed. This difference in speed between the free and bound wave components results in spatial variations in the root-mean-square (rms) free-surface fluctuations, for instance obscuring the interpretation of the results from models with a movable bed.

The problem of reproducing the subharmonics correctly up to second order, for long-crested random waves in the laboratory, has been solved for translating wave boards by Sand (1982), and for translating and rotating wave boards by Barthel et al (1983). The reproduction of superharmonics is dealt with by Sand & Mansard (1986), both for translating and rotating wave boards.

Both the sub- and the superharmonic second-order corrections to the wave-board control signal are determined at every frequency by computing an integral over an appropriate frequency range (involving the Fourier transform of the first-order free-surface elevation and a second-order transfer function). The work needed for generating a control signal correct up to second order is thus proportional to the square of the work needed for generating the first-order signal.

Since most engineering applications deal with sea conditions characterized by quite narrow-banded spectra, the perturbation method of multiple scales is an alternative to generate second-order long-crested random waves in the laboratory. All operations to compute the second-order control signal from the first-order free-surface elevation can be performed in the time domain, and involve only a few simple algebraic operations on the first-order free-surface signal. Therefore, the work needed for generating the second-order control signal is proportional to and only slightly more than the work for generating the first-order signal.

The application of the perturbation method of multiple scales for the present random-wave generation problem, is very similar to the use of the same method by Agnon & Mei (1985) and Agnon, Choi & Mei (1988) for determining the slow-drift motion of two-dimensional bodies in beam seas.

In this paper we first consider some aspects of the usefulness of the narrow-band approximation, for coastal and ocean engineering applications. Next, the perturbation method of multiple scales is applied to the present problem of generating second-order wave-board control signals. Here, we only present results for the subharmonic bound-wave corrections, and not for the superharmonics.

2 Applicability of narrow-band approximation

The accuracy of the multiple-scales method increases as the spectral width decreases. The errors, introduced by the use of the narrow-band approximation in the multiple-scales approach, should be small for the wave spectra normally used in coastal and ocean engineering. In order to get some indication of the usefulness of the multiple-scales perturbation-series method, some comparisons

were made between second-order free-surface elevation spectral densities obtained with the multiple-scales perturbation-series method, as described by Mei (1989, Chapter 12), and those obtained by a full second-order theory, as described by Laing (1986). This comparison only gives an indication of the accuracy, since a non-linear random process is not fully characterized by its autospectrum.

Here, we consider gravity waves on the free surface of a fluid domain of initially constant depth h . The fluid is assumed to be homogeneous, inviscid and incompressible, and the flow is assumed to be irrotational. Surface tension effects and effects of the air above the free surface are neglected. The flow can be described by a velocity potential Φ , with the fluid velocity vector equal to the gradient of the velocity potential.

The perturbation method of multiple scales was used to simulate a finite duration realization of the second-order free-surface elevation in the time domain. The free-surface elevation $\zeta(x, t)$ and the velocity potential $\Phi(x, z, t)$ are expanded into perturbation series:

$$\begin{aligned}\zeta &= \sum_{n=1}^{\infty} \varepsilon^n \zeta_n(x, t), \\ \Phi &= \sum_{n=1}^{\infty} \varepsilon^n \phi_n(x, z, t),\end{aligned}\tag{1}$$

with x the horizontal space coordinate, positive in the wave propagation direction, z the vertical space coordinate, with $z > 0$ above the still water elevation. The time coordinate is denoted by t and ε is a small non-linearity parameter proportional to the wave slope.

Because we are considering propagating wave phenomena, the terms from the perturbation series are expanded into harmonic functions. The amplitudes of the harmonic functions are assumed to vary only slowly in space and time, i.e. the carrier waves are assumed to have narrow-banded spectra. This slow modulation is formalized by the introduction of fast coordinates (x_0, t_0) and a cascade of slow coordinates $(x_1, t_1), (x_2, t_2), \dots$ in the horizontal space and the time direction:

$$\begin{aligned}x_0 &= x, & x_1 &= \varepsilon x, & x_2 &= \varepsilon^2 x_2, \dots, \\ t_0 &= t, & t_1 &= \varepsilon t, & t_2 &= \varepsilon^2 t_2, \dots,\end{aligned}\tag{2}$$

where it has been assumed that the modulation effects are of the same order as the non-linearity effects.

The (quadratic) non-linearity of the problem, due to the non-linear free-surface boundary conditions, introduces higher harmonics into the higher-order solutions:

$$\begin{aligned}\zeta &= \sum_{n=1}^{\infty} \varepsilon^n \sum_{m=-n}^{+n} \zeta^{(n,m)} E_0^m, \\ \Phi &= \sum_{n=1}^{\infty} \varepsilon^n \sum_{m=-n}^{+n} \phi^{(n,m)} E_0^m,\end{aligned}\tag{3}$$

with:

$$E_0 = e^{ix_0}, \quad \chi_0 = k_0 x_0 - \omega_0 t_0, \tag{4}$$

and

$$\begin{aligned} \zeta^{(n,m)} &= \zeta^{(n,m)}(x_1, x_2, \dots; t_1, t_2, \dots), \\ \phi^{(n,m)} &= \phi^{(n,m)}(x_1, x_2, \dots; z; t_1, t_2, \dots), \end{aligned} \tag{5}$$

expressing the slow variation of these complex-valued amplitude functions $\zeta^{(n,m)}$ and $\phi^{(n,m)}$. In (4), k_0 is the carrier wave number and ω_0 is the carrier-wave angular frequency. Because ζ and Φ are real-valued functions, $\zeta^{(n,-m)}$ and $\phi^{(n,-m)}$ have to be the complex conjugates of respectively $\zeta^{(n,m)}$ and $\phi^{(n,m)}$.

The solution of both the first-order and the second-order problem can for instance be found in Mei (1989, Chapter 12):

$$\begin{aligned} \zeta_1 &= \frac{1}{2} (Ae^{ix_0} + *), \\ \phi_1 &= \phi^{(1,0)}(x_1, t_1) - \frac{1}{2} \frac{g \operatorname{ch} Q}{\omega_0 \operatorname{ch} q} (iAe^{ix_0} + *), \end{aligned} \tag{6}$$

and

$$\begin{aligned} \zeta_2 &= \left\{ -\frac{1}{g} \frac{\partial \phi^{(1,0)}}{\partial t_1} - \frac{\omega_0^2}{4g \operatorname{sh}^2 q} |A|^2 \right\} + \\ &\quad + \frac{k_0 \operatorname{ch} q}{8 \operatorname{sh}^3 q} (2 \operatorname{ch}^2 q + 1) (A^2 e^{2ix_0} + *), \\ \phi_2 &= \phi^{(2,0)} - \frac{1}{2} \frac{g \operatorname{ch} Q}{\omega_0 \operatorname{ch} q} \left(\frac{1}{\omega_0} + \frac{q \operatorname{th} q - Q \operatorname{th} Q}{k_0 C_g} \right) \left(\frac{\partial A}{\partial t_1} e^{ix_0} + * \right) + \\ &\quad - \frac{3}{16} \frac{\omega_0 \operatorname{ch} 2Q}{\operatorname{sh}^4 q} (C A^2 e^{2ix_0} + *), \end{aligned} \tag{7}$$

with $q = k_0 h$, $Q = k_0(z+h)$, $C_g = d\omega_0/dk_0$ the group velocity, g the gravitational acceleration, $A(x_1, t_1)$ the complex-valued amplitude of the carrier waves and an asterisk (*) denoting the complex conjugate of the preceding term. We have chosen $\zeta^{(2,1)}$ equal to zero, i.e. the first-order solution ζ_1 completely describes the free-surface elevation spectral density near the peak frequency. The wave number k_0 is related to the angular frequency ω_0 by the linear theory dispersion relation:

$$\omega_0^2 = g k_0 \operatorname{th} q, \tag{8}$$

and further use has been made of

$$\frac{\partial A}{\partial t_1} + C_g \frac{\partial A}{\partial x_1} = 0, \tag{9}$$

which is correct up to second order.

The second-order correction (7) to the free surface elevation ζ still contains $\phi^{(1,0)}$. This is determined from the solvability condition for the third-order zeroth-harmonic $(n, m) = (3, 0)$ problem, see e.g. Mei (1989, Chapter 12), and assuming

that the waves propagate according to Stokes's second definition of wave celerity (i.e. the mean mass flux through a vertical plane perpendicular to the wave propagation direction is equal to zero), resulting in $\langle \zeta \rangle = 0$, with $\langle \cdot \rangle$ denoting a time average. The second-order correction ζ_2 becomes:

$$\zeta_2 = \frac{1}{2} \frac{g}{C_g^2 - gh} \left\{ \frac{C_g}{C_0} + \frac{q}{\text{sh } 2q} \right\} (|A|^2 - \langle |A|^2 \rangle) + \frac{k_0 \text{ch } q}{8 \text{sh}^3 q} (2 \text{ch}^2 q + 1) (A^2 e^{2i\chi_0} + *), \quad (10)$$

with $C_0 = \omega_0/k_0$ the phase velocity.

Equations (6) & (10) are used to simulate part of a realization of the second-order random free-surface elevation. The first-order complex-valued random wave signal $A \exp(i\chi_0)$ is generated from a given first-order free-surface elevation spectrum with the random-amplitude/random-phase method (Tucker et al.; 1984).

The second-order free-surface spectrum can be computed without making the narrow-band approximation with the formulations of Laing (1984). The (one-sided) non-linear free-surface elevation spectrum $S_{\zeta\zeta}(\omega)$ is expanded into a perturbation series:

$$S_{\zeta\zeta}(\omega) = \sum_{n=1}^{\infty} \varepsilon^n S_{\zeta\zeta}^{(n)}(\omega), \quad (11)$$

of which we consider only the first two terms. For a given first-order spectrum $S_{\zeta\zeta}^{(1)}(\omega)$, the second-order correction $S_{\zeta\zeta}^{(2)}(\omega)$ becomes:

$$S_{\zeta\zeta}^{(2)}(\omega) = \int_{\frac{1}{2}\omega}^{\infty} D_{20}(\omega, \omega') S_{\zeta\zeta}^{(1)}(\omega') S_{\zeta\zeta}^{(1)}(\omega' - \omega) d\omega', \quad (12)$$

with $D_{20}(\omega, \omega')$ the second-order transfer function, given by:

$$D_{20} = \frac{2 (D_2(\omega, \omega'))^2}{g^2 (1 - \omega^2/g\kappa \text{th } \kappa h)^2}, \quad (13)$$

$$D_2 = \frac{1}{2} \left\{ (\omega')^2 + (\omega - \omega')^2 + \omega'(\omega - \omega') - \omega'(\omega - \omega') \coth k'h \coth(\kappa - k')h + \omega\omega' \coth \kappa h \coth k'h + \omega(\omega - \omega') \coth \kappa h \coth(\kappa - k')h \right\}, \quad (14)$$

with κ the wave number of the bound waves, and:

$$\begin{aligned} (\omega')^2 &= gk' \text{th } k'h, \\ (\omega - \omega')^2 &= g(\kappa - k') \text{th } (\kappa - k')h, \end{aligned} \quad (15)$$

the dispersion relationships for the free waves. Equation (12) shows that an integral over all frequency pairs has to be computed, in order to obtain the second-order spectrum.

Both descriptions of the second-order free surface elevation, i.e. the multiple-scales perturbation method as well as the full second-order theory in the frequency domain, include the subharmonic as well as superharmonic bound waves. Both methods were used to obtain second order spectra, assuming the first-order spectrum to be of JONSWAP shape:

$$S_{\zeta\zeta}^{(1)}(f) = \frac{\beta H_{rms}^2}{f_p} \left(\frac{f}{f_p}\right)^{-5} \exp\left[-\frac{5}{4}\left(\frac{f}{f_p}\right)^{-4}\right] \gamma^{-\frac{1}{2}} \left(\frac{f-f_p}{\sigma f_p}\right)^2, \quad (16)$$

with $f = \omega/(2\pi)$ the frequency, H_{rms} the rms wave height, f_p the spectral peak frequency, γ the peak enhancement factor, σ the peak width parameter and β a form factor chosen in such a way that $H_{rms}^2 = 8 \int_0^\infty S_{\zeta\zeta}^{(1)}(f) df$.

The results of three simulations will be shown, all with a rms wave height $H_{rms} = 0.7062[m]$, a peak frequency $f_p = 0.25[Hz]$, a still water depth $h = 3[m]$, and with the mean JONSWAP values for σ , i.e. $\sigma = 0.07$ for $f < f_p$ and $\sigma = 0.09$ for $f \geq f_p$. The simulation with the multiple-scales perturbation method in the time domain had a duration of 6400[s] and a sample rate of 5.12[Hz]. The following three values for the peak enhancement factor γ were used:

$\gamma = 20$, a very narrow-banded first-order spectrum,

$\gamma = 3.3$, the mean JONSWAP value, and

$\gamma = 1$, the Pierson-Moskowitz spectrum.

Figures 1-3 show a comparison between the autospectra of the free-surface elevation, obtained from the multiple-scales perturbation method and from the full second-order theory. The relative differences between both approaches become larger when the spectral width increases, and are of the order of 10% of the square root of the spectral density (a measure for corresponding wave amplitude) near $f = 0.02[Hz]$, where the subharmonic spectral density is high. It should also be noted that the relative importance of the bound long waves decreases as the spectral width increases. The difference between the spectrum obtained from the multiple-scales perturbation-series simulation and the theoretical first-order spectrum is due to the random-amplitude approach during the generation of the first-order signal and the finite duration of the numerical simulation (therefore also H_{rms} , obtained from finite-duration realizations, is a random variable). Since the mean free-surface elevation is equal to zero, the spectral density falls off near $f = 0[Hz]$ for the spectra obtained from the numerical simulation, but is not exactly equal to zero due to the computational method used for obtaining the spectra (Fast Fourier Transform on half-overlapping segments, with Van Hann data window).

The deviations, due to the narrow-band approximations implied by the use of the multiple-scales perturbation-series method, were considered to be very acceptable for the spectra commonly used in coastal and ocean engineering.

3 Second-order random-wave generation method

The generation of subharmonic waves, both bound and free waves, is described by Agnon & Mei (1985) in their study of the small-amplitude slow-drift motion due to beam seas of a two-dimensional rectangular block, sliding over the sea bed. Agnon, Choi & Mei (1988) extended this analysis to the case of floating two-dimensional cylinders undergoing both small- and large-amplitude slow-drift motions ('large' meaning motions comparable to or even greater than the motions at the carrier-wave frequency). Here, we use the results of Agnon & Mei (1985) for the determination of the low-frequency wave-board control signal, in such a way that only bound long waves are generated, and no spurious free long waves.

The horizontal wave-board position is denoted by $X(t)$, and the still position is at $x = X = 0$. As in (1), the free-surface elevation $\zeta(x, t)$, the velocity potential $\phi(x, z, t)$, and now also the wave-board position $X(t)$ are expanded into perturbation series:

$$\begin{aligned}\zeta &= \sum_{n=1}^{\infty} \varepsilon^n \zeta_n(x, t), \\ \Phi &= \sum_{n=1}^{\infty} \varepsilon^n \phi_n(x, z, t), \\ X &= \sum_{n=1}^{\infty} \varepsilon^n X_n(t).\end{aligned}\tag{17}$$

The terms in the perturbation series are again expanded into harmonic functions, as in (3). We introduce a cascade of slow variables, cfm. (2). However, now the amplitudes of the harmonic functions vary fast in space near the wave board due to the presence of evanescent modes. Therefore, the solution is assumed to be of the following form:

$$\begin{aligned}\zeta &= \sum_{n=1}^{\infty} \varepsilon^n \sum_{m=-n}^{+n} \zeta^{(n,m)} e^{-im\omega_0 t_0}, \\ \Phi &= \sum_{n=1}^{\infty} \varepsilon^n \sum_{m=-n}^{+n} \phi^{(n,m)} e^{-im\omega_0 t_0}, \\ X &= \sum_{n=1}^{\infty} \varepsilon^n \sum_{m=-n}^{+n} X^{(n,m)} e^{-im\omega_0 t_0},\end{aligned}\tag{18}$$

with:

$$\begin{aligned}\zeta^{(n,m)} &= \zeta^{(n,m)}(x_0, x_1, x_2, \dots; t_1, t_2, \dots), \\ \phi^{(n,m)} &= \phi^{(n,m)}(x_0, x_1, x_2, \dots; z; t_1, t_2, \dots), \\ X^{(n,m)} &= X^{(n,m)}(t_1, t_2, \dots),\end{aligned}\tag{19}$$

i.e. the harmonic functions $\zeta^{(n,m)}$ and $\phi^{(n,m)}$ are also functions of x_0 , and it is not assumed that the first-order solution only contains propagating waves $A \exp [i(k_0x_0 - \omega_0t_0)]$, but also evanescent modes fixed to the wave board.

The derivation of the first-order solution and the second-order subharmonic solution can be found in Agnon & Mei (1985), including how to remove the evanescent mode contributions from the subharmonic solution. These derivations will not be repeated here, but we only present the results for our problem of second-order wave-board control. The first-order first-harmonic solution is:

$$\begin{aligned}
 \zeta^{(1,1)} &= \frac{1}{2} A(x_1 - C_g t_1) e^{ik_0 x_0} + \\
 &\quad - i \frac{\omega_0 C_g}{C_0} \frac{1}{2} A(-C_g t_1) \sum_{l=1}^{\infty} \frac{1}{k_l} \frac{1}{C_g - \frac{1}{2}(q_0^2 + q_l^2)/(k_D h)} e^{-k_l x_0}, \\
 \phi^{(1,1)} &= -i \frac{g \operatorname{ch} Q_0}{\omega_0 \operatorname{ch} q_0} \frac{1}{2} A(x_1 - C_g t_1) e^{ik_0 x_0} + \\
 &\quad - \frac{g C_g}{C_0} \frac{1}{2} A(-C_g t_1) \sum_{l=1}^{\infty} \frac{1}{k_l} \frac{\cos Q_l}{\cos q_l} \frac{1}{C_g - \frac{1}{2}(q_0^2 + q_l^2)/(k_D h)} e^{-k_l x_0}, \\
 X^{(1,1)} &= i \frac{C_g}{C_0 \operatorname{th} q_0} \frac{1}{2} A(-C_g t_1),
 \end{aligned}
 \tag{20}$$

with $k_D = \omega_0^2/g$, $q_l = k_l h$, $l = 0, 1, 2, \dots$ and $Q_l = k_l(z + h)$, $l = 0, 1, 2, \dots$. The propagating wave number k_0 and the evanescent-mode wave numbers k_l , for $l = 1, 2, \dots$ satisfy the linear-theory dispersion relationships:

$$\omega_0^2 = \begin{cases} g k_0 \operatorname{th} q_0 & , l = 0, \\ g k_l \tan q_l & , l = 1, 2, \dots \end{cases}
 \tag{21}$$

The first-order zeroth-harmonic solution is:

$$\begin{aligned}
 \zeta^{(1,0)} &= 0, \\
 \phi^{(1,0)} &= \frac{g^2 [2\omega_0 k_0 + C_g(k_0^2 - k_D^2)]}{4\omega_0^2 (C_g^2 - gh)} \left(\int_{-\infty}^{x_1 - C_g t_1} |A(\psi)|^2 d\psi \right), \\
 X^{(1,0)} &= -\frac{g^2}{4\omega_0^2 C_g} \left(\frac{2\omega_0 k_0 + C_g(k_0^2 - k_D^2)}{C_g^2 - gh} + \frac{2\omega_0 k_0}{gh} \right) \times \\
 &\quad \times \int_{-\infty}^{-C_g t_1} (|A(\psi)|^2 - \langle |A|^2 \rangle) d\psi,
 \end{aligned}
 \tag{22}$$

where $X^{(1,0)}$ is the desired subharmonic bound-wave contribution to the wave-board control signal X . Note that $\phi^{(1,0)}$ and $X^{(1,0)}$ are proportional to $|A|^2$, and thus in fact higher-order quantities. This is due to the fact that their derivatives $\partial\phi^{(1,0)}/\partial x_1$ and $\partial X^{(1,0)}/\partial t_1$ are the relevant physical quantities which are second-order quantities within the multiple-scales perturbation-series approach.

From the second-order zeroth-harmonic contribution to the solution, only the $\zeta^{(2,0)}$ -term is needed:

$$\zeta^{(2,0)} = -\frac{1}{g} \left\{ \frac{\partial \phi^{(1,0)}}{\partial t_1} + \left[\left| \frac{\partial \phi^{(1,1)}}{\partial x_0} \right|^2 - k_D^2 |\phi^{(1,1)}|^2 \right]_{z=0} \right\}. \quad (23)$$

In summary, $\zeta^{(1,1)}$, $\phi^{(1,1)}$ and $X^{(1,1)}$ in (20) are the terms proportional to the wave amplitude A , and $\zeta^{(2,0)}$, $\phi^{(1,0)}$ and $X^{(1,0)}$ in (22) & (23) are the subharmonic terms proportional to $|A|^2$.

The first-order random free-surface signal $A \exp(-iC_g t_1)$ is generated with the random-amplitude/random-phase method (Tucker et al.; 1984), for a given first-order free-surface elevation spectrum, as in Section 2. Next the wave-board control signal, correct up to second order, is computed. Required time integrations are performed with the modified midpoint rule, and time differentiation with central finite differences, both of second-order accuracy, i.e. $O(\Delta t^2)$. Also deterministic waves, such as monochromatic and bichromatic waves, can be generated correctly up to second order with these equations.

At the moment, flume tests are performed at Delft University of Technology, for the experimental verification of the second-order wave-board control system.

4 Concluding remarks

The perturbation-series method of multiple scales has been used to derive an efficient method for the generation of second-order random waves in wave flumes with a translating wave board. The method is presented in detail for the subharmonic corrections to the wave-board control signal, but can easily be extended to include the superharmonic corrections.

The amount of work to generate the second-order corrections with the proposed method is proportional to the amount of work to generate the first-order signal. In previously used second-order frequency-domain methods, this amount of work was proportional to the square of the effort for generating the first-order signal.

Furthermore, the narrow-band approximation, implied by the use of the multiple-scales perturbation-series approach, seems to be very acceptable for the first-order spectral shapes most frequently used in coastal and ocean engineering problems.

Acknowledgments

This research has been sponsored by the Netherlands Organization for the Advancement of Research (N.W.O.) and Delft Hydraulics's Long-Term Research Theme for Experimentation Techniques.

The authors wish to thank Mr. L. Verhage for performing the computing analysis and coding of the wave-board control software package, and Mr. H.A.H. Petit for checking the formulas.

References

- Agnon, Y. and Mei, C.C. (1985) "Slow-drift motion of a two-dimensional block in beam seas", *J. Fluid Mech.* **151**, pp. 279-294.
- Agnon, Y., Choi, H.S. and Mei, C.C. (1988) "Slow drift of a floating cylinder in narrow-banded beam seas", *J. Fluid Mech.* **190**, pp. 141-163.
- Barthel, V., Mansard, E.P.D., Sand, S.E. and Vis, F.C. (1983) "Group bounded long waves in physical models", *Ocean Engng.* **10**(4), pp. 261-294.
- Laing, A.K. (1986) "Nonlinear properties of random gravity waves in water of finite depth", *J. Phys. Oceanogr.* **16**(12), pp. 2013-2030.
- Mei, C.C. (1989) "*The applied dynamics of ocean surface waves*", World Scientific Publ., Singapore.
- Sand, S.E. (1982) "Long wave problems in laboratory models", *J. Waterway, Port, Coastal, Ocean Engng.* **108**(WW4), pp. 492-503.
- Sand, S.E. and Mansard, E.P.D. (1986) "The reproduction of higher harmonics in irregular waves", *Ocean Engng.* **13**(1), pp. 57-83.
- Tucker, M.J., Challenor, P.G. and Carter, D.J.T. (1984) "Numerical simulation of a random sea: a common error and its effect upon wave group statistics", *Appl. Ocean Res.* **6**(2), pp. 118-122.

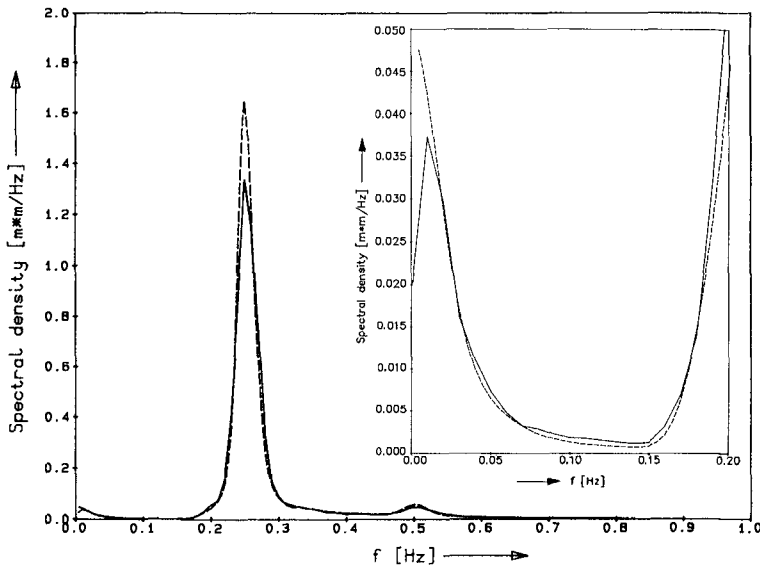


FIGURE 1. Second-order spectral energy density of free-surface elevations ($\gamma = 20$), ——— multiple-scales perturbation-series simulation (Mei; 1989), - - - - full second-order theory (Laing; 1986).

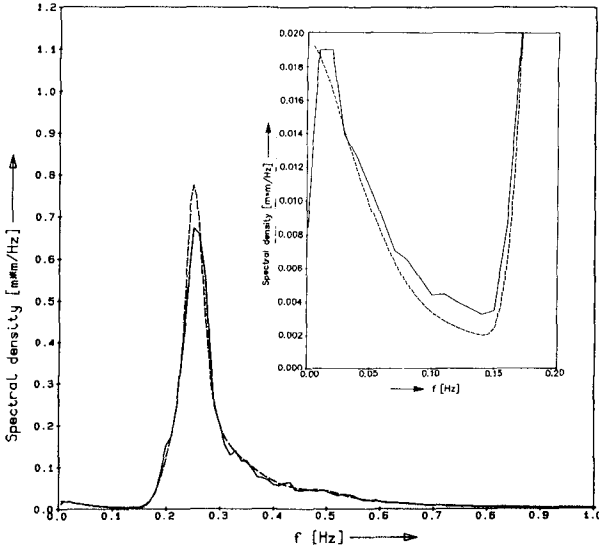


FIGURE 2. Second-order spectral energy density of free-surface elevations ($\gamma = 3.3$; mean JONSWAP spectrum), ——— multiple-scales perturbation-series simulation (Mei; 1989), - - - - full second-order theory (Laing; 1986).

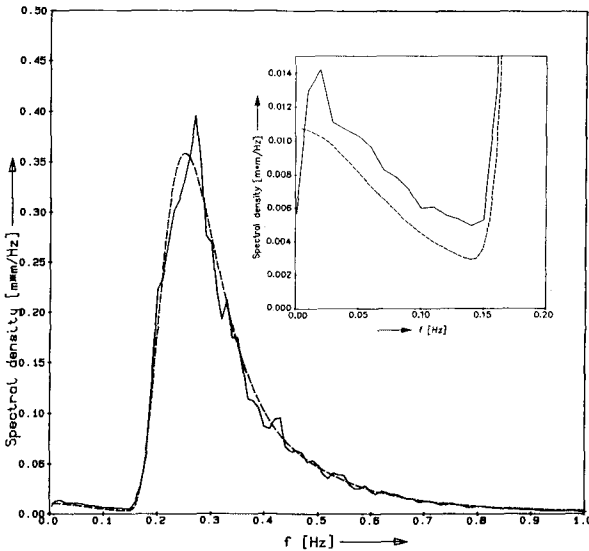


FIGURE 3. Second-order spectral energy density of free-surface elevations ($\gamma = 1$; Pierson-Moskowitz spectrum), ——— multiple-scales perturbation-series simulation (Mei; 1989), - - - - full second-order theory (Laing; 1986).